Nonisothermal Cure Kinetics of Diglycidylether of Bisphenol-A/Amine System Reinforced with Nanosilica Particles

M. Ghaemy, S. M. Amini Nasab, M. Barghamadi

Department of Chemistry, Mazandaran University, Babolsar, Iran

Received 19 September 2006; accepted 22 December 2006
DOI 10.1002/app.25994
Published online in Wiley InterScience (www.interscience.wiley.com).

ABSTRACT: Epoxy-silica nanocomposites were obtained from directly blending diglycidylether of bisphenol-A (DGEBA)-based epoxy and nanoscale silica (NS) and then curing with 4,4′-diaminodiphenylamine (DDA). The effect of amount of nanosilica (NS) particles as catalyst on the mechanism and kinetic parameters of cure reaction of DGEBA/DDA system was studied. The kinetics parameters were obtained from nonisothermal differential scanning calorimeter (DSC) data using the Kissinger and Ozawa equations. The exothermic peak was shifted toward lower temperatures in DGEBA/DDA/NS system with increasing the amount of nanoslica particles. However, the existence of NS particles with hydroxyl groups in the structure in the mixture of DGEBA/DDA catalyzes the cure reaction and increases the rate constant. The activation energy of cure reaction of DGEBA/DDA system obtained from two methods were in good agreement, and showed a decrease when NS particles were present in the mixture. The mechanism of reaction of DGEBA with DDA was carried out by isothermal curing in the oven at 130°C and measuring the disappearance peak of epoxide group at 916 cm^{-1} using FTIR. The diffusive behavior of two systems was investigated during water sorption at 25°C and the experimental results fitted well to Fick's law. Diffusion coefficient of cured sample from DGEBA/DDA/10% NS blend decreased in comparison with the sample without NS particles. J Appl Polym Sci 104: 3855–3863, 2007

Key words: nanosilica; epoxy; nanocomposites; DSC; FTIR; kinetic

INTRODUCTION

The physical and chemical properties of materials in nanoscale have been found to be very different from the properties of the analogous bulk material. This specific character provides the motivation of developing materials having novel functions and properties from the existing substances. Mixing the nanoscale particles with polymeric materials provides a convenient approach to form organic–inorganic hybrid materials. Hybrid materials, also known as nanocomposites, having both inorganic and organic components are interesting substances from the standpoint of their potentially increased performance capabilities relative to those either of their nonhybrid species. The property of a composite material, certainly, is depending on the properties of the individual components and also significantly on the interfacial properties. Using nanoscale fillers in formation of nanocomposites exhibited high interfacial areas and exceptional properties.[1] The new functional nanomaterials are now one of the flourishingly attractive subjects in modern science and technology. The utility of nanoscale particles as reinforcement into linear thermoplastics[2–8] or thermoset networks[9–12] shows attractive properties relative to their thermal, oxidative, and dimensional stability and this process provides many polymer resins for high performance engineering applications.

To predict the morphology developed by the phase separation of rubber-rich phase during polymerization of epoxy resin with amines, and it is necessary to know the reaction kinetics of the crosslinked polymer system. Although the chemistry involve in the epoxy curing process is rather complex, but understanding the mechanisms and kinetics of the cure reactions are essential for a better knowledge of structure-property relationships. Curing kinetics models are generally developed by analyzing experimental results obtained by DSC both in the isothermal and dynamic modes extensively, assuming a cure and extent of reaction.[13–17]

Moisture/water is the most commonly encountered service environment, and must be considered a critical factor in determining the long-term durability of polymers especially adhesively bonded joints. The crosslinked network structure of epoxy resin with highly

Correspondence to: M. Ghaemy (ghaemy@umz.ac.ir).

polar nature of the specific functional groups, such as hydroxyl and amines, is expected to have water uptake as bound water and as free water, which becomes crucial when long-term properties of the material needed. The absorbed moisture in epoxy resin may act as plasticizer with resultant depression in T_g and the elastic modulus E'[18,19] can cause permanent chemical and physical changes[20,21] by microcavities or crazes in polymeric materials, which can further accelerate the moisture diffusion. Several research studies[22–25] have predicted the extent of plasticization of neat and reinforced epoxy resins. It has also been pointed out that these predictions are questionable[26] or only qualitatively applicable. Studies[27] also showed that absorbed water cannot be totally removed by thermal annealing and the residual water in the adhesive is believed to be the one, which is strongly bonded to polar sites. Water can exist in two ways: (1) as free water is present in capillaries and microcavities within the polymer and (2) as bound water is characterized by strong interactions with the matrix.

In this investigation, we studied the reaction kinetics and mechanism of two systems: DGEBA (diglycidylether of bisphenol-A)/DDA (4,4′-diaminodiphenylamine) and DGEBA/DDA/NS (nanoscale silica) using nonisothermal DSC technique. To calculate the kinetic parameters, DSC data under dynamic conditions were introduced to the Kissinger and Ozawa equations. The effect of amount of NS up to 20% loading on the rate of cure reaction of DGEBA with DDA is reported. The cure reaction mechanism and conversion of epoxide group in both systems were studied and confirmed by using isothermal mode FTIR analysis. The other objective of this investigation was to compare the water diffusion of the two systems. Water diffusion in epoxy resin matrices has frequently been represented by Fickian behavior. According to the Fick's second law, the diffusion coefficient D depends on the changes in concentration C of a diffusing substance as a function of time t and position x and is given by:

$$\frac{\partial C}{\partial t} = D\frac{\partial^2 C}{\partial x} \tag{1}$$

EXPERIMENTAL

Apparatus

A Metteler Toledo differential scanning calorimeter (DSC822^e) was used to monitor the exothermic thermograms of crosslinking reaction. The FTIR used was Bruker (Vector 22) and the FTIR spectra of the curing reaction were taken using KBr pellets.

Materials

The epoxy compound used in the study was a DGEBA-based epoxy, Epidian5: Epoxide equivalent 196–208, clear yellow liquid, viscosity (at 25°C) 25,000 mPa s, provided from Iran Petrochemical Industry (Khuzestan, Iran). DDA/sulfate was purchased from Fluka (Germany). DDA was obtained from hydrolyzing of DDA/sulfate mixture according to the procedure given below. DDA is completely soluble in the resin at temperatures above $\sim$ 50°C. Nanosilica was purchased from Nissan Chemical (Tokyo, Japan). Characteristics data for NS particles are absorption peaks at 3397 and 1106 cm^{-1} related to hydroxyl and Si—O—Si groups. NS particles were dissolved in CD_3—S(O)—CD_3. H NMR spectra were recorded at room temperature on a Varian Unity 200 Spectrometer, and showed a wide singlet at 4.1 ppm related to the hydroxyl group. The chemical structures of the compounds used in this study are shown in Scheme 1.

DGEBA (composed principally of two homologs n = 0 and n = 1).

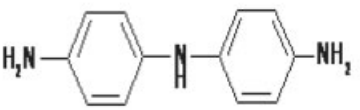

DDA

Scheme 1

TABLE I
DSC Scanning Data for Blends Cured at Different Heating Rates

Sample	q (°C/min)	T_p (K)	$1/T_p \times 10^3$ (K^{-1})	ln q	$-\ln (q/T_p^2)$
DGEBA/DDA	5	391.38	2.5551	1.61	10.3300
	10	414.41	2.4131	2.30	9.7511
	15	424.91	2.3534	2.71	9.3957
	20	435.23	2.2976	3.00	9.1560
DGEBA/DDA/10%NS	5	377.15	2.6515	1.61	10.255
	10	396.77	2.5203	2.30	9.6641
	15	404.24	2.4738	2.71	9.2959
	20	424.57	2.3553	3.00	9.1064

Hydrolysis of DDA/sulfate

DDA/sulfate was suspended in 500 mL of water in a 1-L beaker equipped with a stirrer, and the mixture is slowly neutralized by the addition of 2.5*N* sodium hydroxide. In the course of the neutralization, the salt dissolves and the free base separates. The DDA is collected on a Buchner funnel, washed with water, and dried under reduced pressure. The final product was dissolved in hot water by slowly addition of ethanol to give a clear solution. The solution was stored in a refrigerator to give needlelike crystals with the melting point of 158°C.

Sample mixing

The stoichiometric amounts of the curing agent (DDA) were calculated through the number of active amino hydrogen. DDA with a molar mass of 199 g/mol and five active hydrogen atoms in the molecule represents 40 g for one mole of active hydrogen. This figure is in the stiochiometric equivalent of the eew and, hence, for every about 200 g of DGEBA, 40 g DDA was used as a curing agent. NS of 5, 10, 15, and 20% based on the weight of DGEBA were used. Therefore, samples of DGEBA containing the required amount of NS particles were mixed at 50°C to reduce the viscosity of the resin and thoroughly stirred on a magnetic stirrer for 20 min to give a homogeneous and uniform blend. Stoichiometric amount of curing agent was added to the blend and mixed completely before using for DSC test.

Samples for water absorption test were prepared from the blend in the form of discs in the range of 0.7–1.2 mm thickness in aluminum cells and heated in an oven at 130°C for 2 h. The samples were introduced in flasks containing water, and were kept there for different periods of times at room temperature before being studied.

DSC analysis

A 5–6 mg of the uniform viscous mixture was put into a DSC sample pan and covered with an aluminum lid and closed tightly under pressure. The sample pan was placed in the DSC sample cell at ambient temperature and an empty pan was also placed in the DSC reference cell, and it was heated according to the program of a constant heating rate from room temperature to 300°C. The heating rates were 5, 10, 15, and 20°C/min under nitrogen purge gas.

FTIR analysis

FTIR analysis was carried out to study mechanism of cure reaction in DGEBA/DDA and DGEBA/DDA/NS systems. A thin layer of the uniform viscous mixture on a KBr disc was heated in an oven at 130°C for various times and the partially cured sample was analyzed by FTIR spectroscopy from 4000 to 700 cm^{-1}. The characteristic band for epoxide group (916 cm^{-1}) was recorded and compared with —C=C— stretching of aromatic rings at 1610 cm^{-1} (spectrum C).

RESULTS AND DISCUSSION

Table I shows the DSC scanning data obtained for DGEBA/DDA and DGEBA/DDA/10% NS systems at different heating rates (5, 10, 15 and 20°C/min). Figure 1 shows dynamic DSC curves for DGEBA/

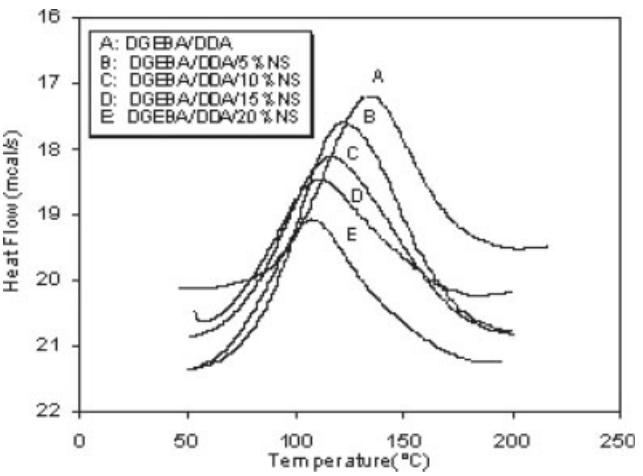

Figure 1 Typical DSC thermograms of cure reaction of DGEBA/DDA with different amounts of NS at 10°C/min.

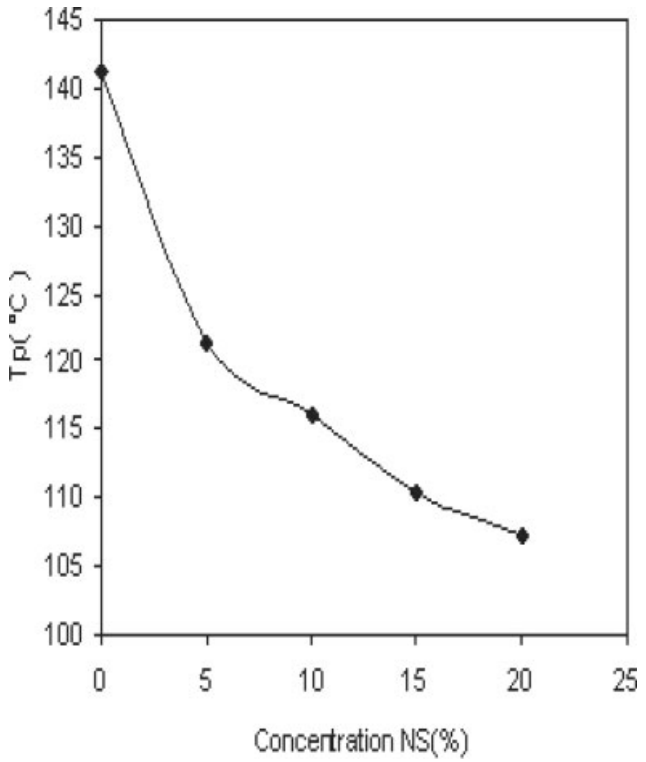

Figure 2 Effect of amount of NS on the maximum temperature of the exothermic peaks.

DDA/NS systems at different concentrations of NS particles and at the same heating rate. The maximum temperature of exothermic peak (T_p), as well as the exothermic peaks, for DGEBA/DDA/NS system was shifted to a low temperature region with increasing amounts of the NS particles. The effect of amounts of NS on T_p is shown in Figure 2 and Table II. It can be seen that the first 5% of NS had shifted the exothermic peak 20°C to the lower temperature. In comparison with the exothermic peak of DGEBA/DDA system, the difference in the maximum is attributed to the increased rate of the cure reaction for DGEBA/DDA/NS system. It was reported[28] that nanoscale colloidal silica particles can act as a curing agent for epoxy if tin chloride was used as catalyst or when the amount of nanosilica exceeded 20 phr. In our system with 20% NS, no cure reaction occurred without addition of DDA. This difference proposes, in DGEBA/DDA/NS system, that NS particles catalyze the reaction; therefore, maximum cure temperature was decreased. The reactivity between NS particles and epoxy DGEBA was not observed with simple heating of the blended mixture of DGEBA with different concentrations of NS particles up to 20%, the reaction did not occur and left a muddylike product. Blend of DGEBA/20% NS did not show the exothermic behavior even at temperatures as high as 300°C. The reactivity difference between DGEBA/NS and DGEBA/NS/DDA systems was clearly observed with DSC thermograms. For the DGEBA/10% NS/DDA mixture, the exothermic behavior was observed starting at ~ 70°C and showed an exothermic peak at 116°C while the blend without NS started the exothermic peak almost at the same temperature but reached to its maximum at ~ 133°C. Therefore, in this system, the hydroxyl groups of NS act as catalyst in reaction between epoxide group and primary or secondary amine groups. For both systems, the exothermic peak showed a very steep slope, meaning that the cure reaction took place rapidly in a short temperature range.

The mechanism of cure reaction was confirmed by FTIR analysis. Figure 3 shows the FTIR spectra of DGEBA cured with 20 phr DDA in the oven at 130°C from 0 (spectrum A) to 60 min (spectrum B). The —C=C— stretching of aromatic ring at 1610 cm^{-1} (spectrum C) was taken as a reference peak for the normalization of the epoxy absorption peak. In spectrum A, the characteristic band of the epoxy ring vibration of DGEBA appeared at 916 cm^{-1}, and as the cure reaction preceded this characteristic band of the epoxy ring decreased and removed completely at the end of cure reaction. The epoxide groups' conversion against cure time, which has been calculated according to the eq. (2) from FTIR spectra is shown in Figure 4.

$$[E]_t = \frac{[A]_t}{[B]_t} \quad \text{and} \quad \alpha = \frac{[E]_0[E]_t}{[E]_0} \tag{2}$$

where $[A]_t$ and $[B]_t$ are the area under peak for 916 and 1610 cm^{-1}, respectively, and [E] denotes the concentration of epoxide group at time t and the subscript 0 denotes time $t = 0$.

The initial slope of the curves in Figure 4 was steeper but next to that, the slope becomes smaller after a certain amount of time, which could have been due to a diffusion-controlled reaction. The curve for DGEBA/DDA system is less steep in comparison with the curve of DGEBA/DDA/NS system, which is due to the catalytic activity of NS particles; therefore, the rate of reaction in this system was increased. The degree of conversion (α) (Fig. 4) showed autoacceleration in the initial stages, as indi-

TABLE II
DSC Scanning Data for DGEBA/DDA Blend Cured with Different Amounts of NS at 10°C/min

Conc. of NS (%)	T_p (K)	Exothermic heat (J/g)
0	414.41	156.159
5	394.41	259.622
10	389.18	224.341
15	383.57	158.532
20	380.55	156.959

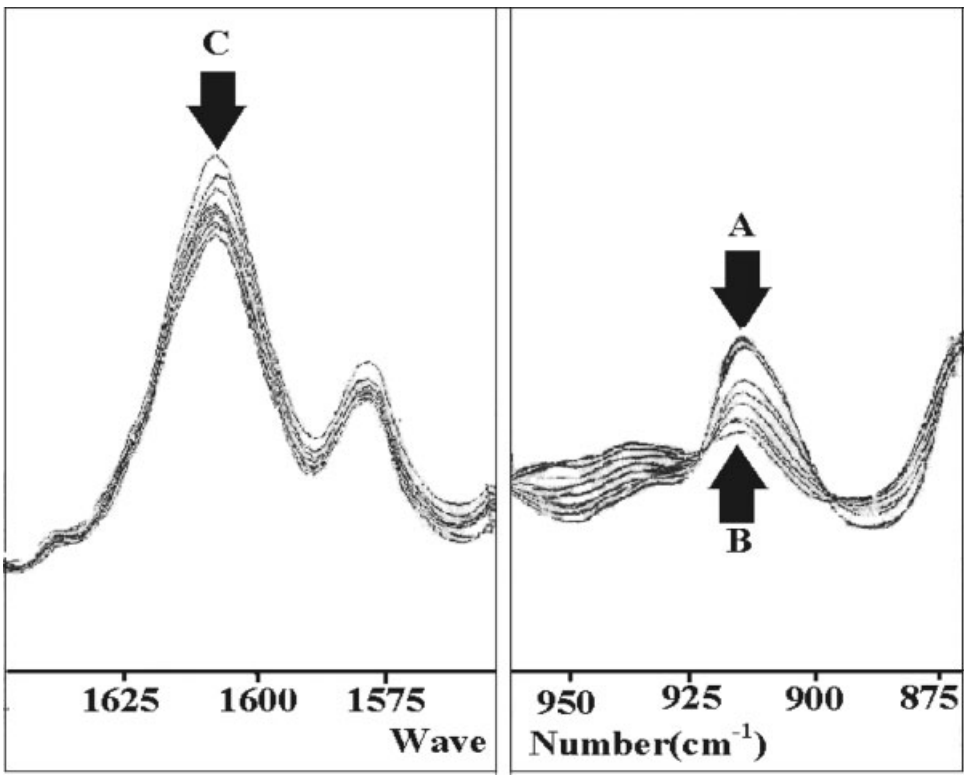

Figure 3 FTIR spectra of mixture of DGEBA and 20 phr DDA during cure reaction at 130°C for 30 min.

cated by the slight positive curvature. Curing thermosetting materials, which generally involve transition of low molecular weight in liquid or rubbery state to an amorphous glassy state with infinite molecular weight, are called vitrification. The chemical kinetics in the region near vitrification is often complicated by diffusion and/or mobility control. In principal, the reaction can proceed to a point ($T_g > T_{\text{cure}}$) where all chain movement ceases and the reaction arrests because of the complete absence of mobility. This leads to a final conversion lower than unity in diffusion-controlled conditions. The ultimate conversion can also be lower because of the fact that the remaining reactive groups cannot meet and react even in the absence of any diffusion hindrance.

The exothermic peak of DSC thermograms is mainly caused by the sum of the reactions shown in Scheme 2: (a) noncatalytic (reactions 1 and 4) or catalytic (reactions 2 and 3) reactions between primary and secondary amines with epoxide groups, which yield secondary and tertiary amines and hydroxyl groups. The catalytic reaction between amine and epoxide groups can be carried out by the catalytic action of hydroxyl groups present in the structure of NS particles and produced during epoxide ring opening reaction. (b) The etherification reactions (reaction 6), which may be neglected for stoichiometric mixtures of epoxy with diamines since the reactivity of the diamines to the epoxide rings is much higher than the hydroxyl groups, can be significant when diamine is lower than the stoichiometric value and at temperatures above 200°C.

However, many equations were developed to investigate the cure kinetics of the epoxy system, including the *n*th-order reaction model, the autocatalytic reaction model, and the diffusion-control

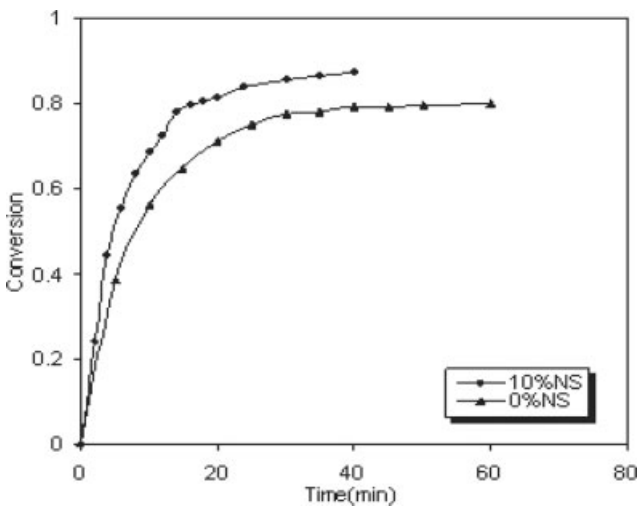

Figure 4 Conversions calculated from FTIR spectra against time of cure reaction at 130°C for DGEBA/DDA and DGEBA/DDA/10% NS systems.

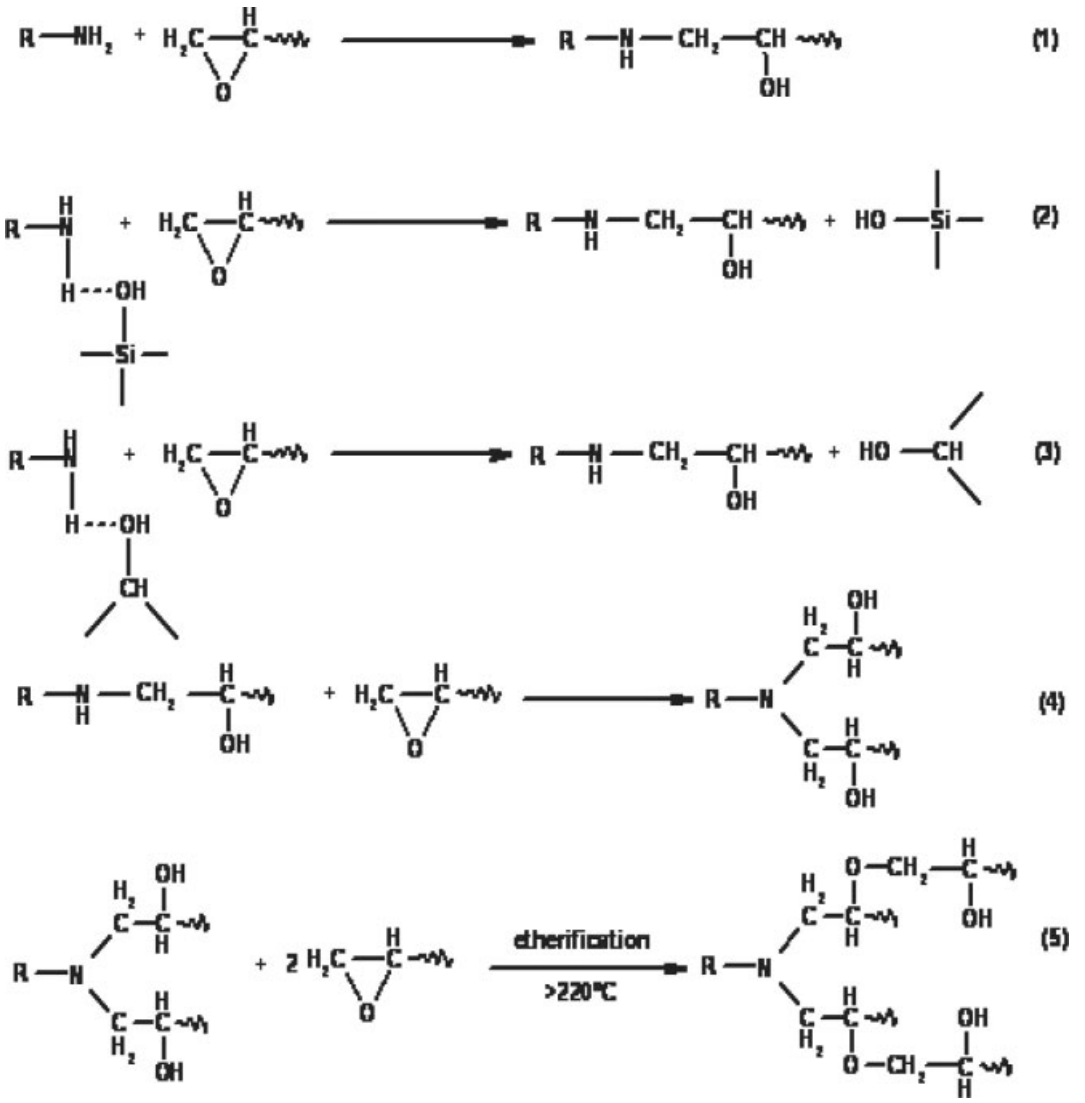

Scheme 2

model. All kinetic models start with the following basic equation:

$$\frac{d\alpha}{dt} = kf(\alpha) \tag{3}$$

or in the integrated form,

$$g(\alpha) = \int \frac{d\alpha}{dt} = \int kdt \tag{4}$$

where $d\alpha/dt$ is the instant cure rate, α is the fractional conversion at a time t k is the Arrhenius rate constant, and $f(\alpha)$ is a functional form of α that depends on the reaction mechanism.

Kissinger derived the following equation[29,30] for when the temperature varies with time at a constant heating rate, $q = dT/dt$:

$$-\ln\left(q/T_p^2\right) = E/RT_p - \ln(AR/E) \tag{5}$$

where q is the heating rate, T_p is the temperature at which $d\alpha/dt$ is maximum, E is the activation energy, R is the gas constant, and A is the pre-exponential factor. This method gives a relatively accurate activation energy and pre-exponential factor by calculating the relationship between $-\ln(q/T_p^2)$ and $1/T_p$.

The data of the fourth and sixth columns (Table I) were introduced to the Kissinger equation, and $-\ln(q/T_p^2)$ versus $1/T_p$ is plotted in Figure 5. The linear plots are expressed by the following equations for DGEBA/DDA and DGEBA/DDA/NS systems, respectively:

$$-\ln\left(q/T_p^2\right) = 4.596 \times 10^3(1/T_p) - 1.395 \quad \text{(DGEBA/DDA)} \tag{6}$$

and

$$-\ln\left(q/T_p^2\right) = 4.003 \times 10^3(1/T_p) - 0.428 \quad \text{(DGEBA/DDA/NS)} \tag{7}$$

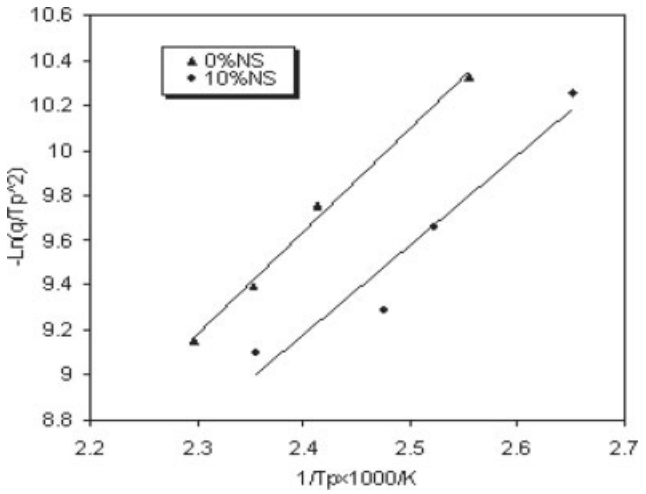

Figure 5 Kissinger plots for DGEBA/DDA system.

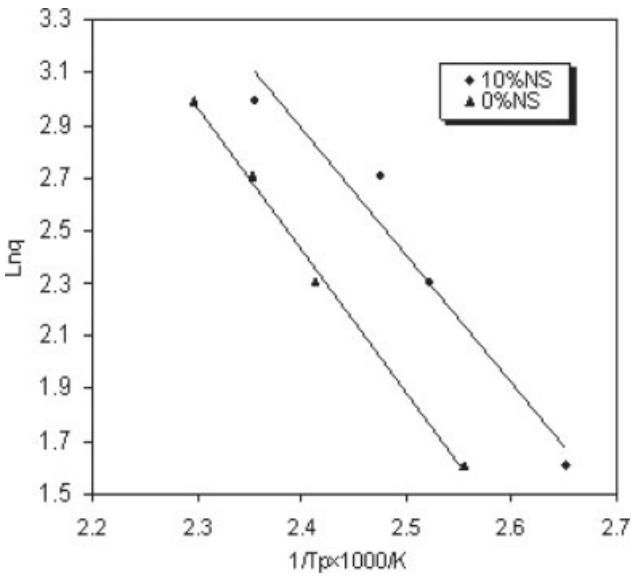

Figure 6 Ozawa plots for DGEBA/DDA system.

The activation energies were calculated from the slope and the pre-exponential factors from the y intersect, and these values were listed in Table III. To compare the cure rate for the two systems, pre-exponential factor and activation energy values are introduced to the following Arrhenius equation to obtain rate constants at a selected temperature and the data are shown in Table III.

$$k = A\exp(-E_a/RT) \tag{8}$$

where k is the rate constant and T is a selected temperature (403 K). The rate constant for DGEBA/DDA/NS system was increased, because hydroxyl groups in the structure of NS particles catalyzed the curing reaction, therefore the activation energy E_a was decreased.

Ozawa-Flynn-Wall method based on Doyle's approximation[31,32] is an alternative method for the calculation of activation energy and is expressed as follows:

$$\ln q = 1/2.303\ \ln q = -0.4567E_a/RT_p + (\log AE_a/R - \log f(\alpha) - 2.315) \tag{9}$$

A plot of $\ln(q)$ versus $(1/T_p)$ should give a straight line with a slope of 1.052 E_a/R (Fig. 6). This can provide activation energy for different levels of conversion (Table III). Activation energies from Ozawa and Kissinger equations were in good agreement, and Ozawa activation energy confirmed the Kissinger calculations.

TABLE III
Values of Kinetic Parameters of Cure Reaction

Sample	[a]E_a (kJ/mol)	[b]E_a (kJ/mol)	A (min^{-1})	[c]K (min^{-1})
DGEBA/DDA	38.215	42.830	1.85×10^4	0.206
DGEBA/DDA/ 10% NS	33.284	37.956	6.14×10^3	0.298

[a] Kissinger's method.
[b] Ozawa's method.
[c] Arrhenius rate constant at 403 K.

The crosslinked network structure of epoxy resin with highly polar nature of the specific functional groups, such as hydroxyl and amines, are expected to have water uptake as bound water and as free water, which becomes crucial when long-term properties of the material needed. Water diffusion in epoxy resin matrices has frequently been represented by a Fickian behavior (Fick's second law), whose mathematical expression is represented by eq. (1). The diffusion coefficient can be calculated from the slope of the linear region of the diffusion curve that is obtained fitting experimental values of water uptake M_t (%) vs. $t^{1/2}$. The total amount of water diffusing in the crosslinked network material M_t as a function of time is given by the integral of the solution of eq. (1) across the thickness h of the sample.

$$\frac{M_t}{M_{\max}} = 1 - \frac{8}{\pi^2}\sum_{n=0}^{\infty}\frac{1}{(2\pi+1)^2} \times \exp\left[-D(2n+1)^2\frac{\pi^2 t}{h^2}\right] \tag{10}$$

where $M_{\max}$ is the maximum amount of the diffusing water at infinite time.

The curve can be divided in two parts.

If $D_t/h^2 > 0.05$ [eq. (10)] can be rewritten as the following expression:

$$\frac{M_t}{M_{\max}} = 1 - \frac{8}{\pi^2}\exp\left[-\left(\frac{Dt}{h^2}\right)\pi^2\right] \tag{11}$$

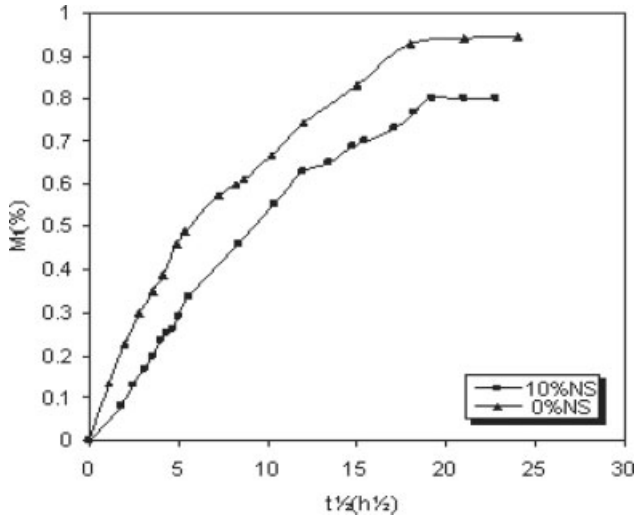

Figure 7 Water diffusion curves of two systems at 25°C.

If $D_t/h^2 \leq 0.05$ (or $M_t/M_{max} < 0.6$) [eq. (10)] can be simplified and written as

$$\frac{M_t}{M_{max}} = \frac{4}{h\sqrt{\pi}}\sqrt{Dt} \tag{12}$$

The M_t (%) values were obtained from the water uptake of three samples after exposure to identical conditions. The relative weight increase in each sample was calculated as

$$\Delta m_{ti} = (m_{ti} - m_{0i})/m_{0i} \times 100 \tag{13}$$

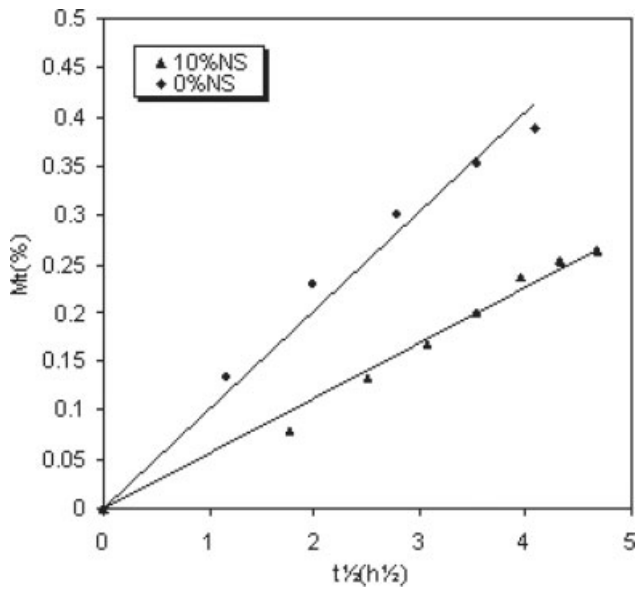

Figure 8 Linear regions of the water diffusion curves at the 25°C.

TABLE IV
Diffusion Coefficients

Sample	Da (10^{-9} m^2/s)
DGEBA/DDA	6.50
DGEBA/DDA/10% NS	4.45

And the average weight increase is

$$M_t(\%) = \sum_{i}^{3} \Delta m_{ti}/3 \tag{14}$$

Diffusion behavior of DGEBA/DDA and DGEBA/DDA/NS systems at 25°C is shown in Figure 7, where fitting the experimental measurements of M_t (t) against $t^{1/2}$ resulted in curves. The experimental curves were plotted up to the beginning of the equilibrium plateau (three experimental points with similar values within the limits of experimental error). As can be seen, the behavior is similar to that predicted by Fick's law. The features of Fickian diffusion have been described in the literature[33]: (1) sorption curves are linear in the initial stages; and (2) above the linear portions, sorption curves are concave to the abscissa axis. Our experimental results reasonably fulfilled these criteria.

Shape of the curves suggests the beginning of the quasi-equilibrium stages almost after 100 h of exposure.

From the linear fits, in the first step of the M_t (%) vs. $t^{1/2}$ ($h^{1/2}$) curves (Fig. 8), the diffusion coefficients were calculated by means of the following expression:

$$m = \frac{\sqrt{D}4M_{sat}}{h\sqrt{\pi}} \tag{15}$$

where m is the slope of these fittings.

The diffusion coefficients for two systems are given in Table IV. As can be seen, the diffusion coefficient decreases when NS is present in DGEBA/DDA system. The diffusion of higher amount of water into cured DGEBA/DDA material can be because of the existence of more microvoids on the surface of the sample. Addition of nanosilical particles as filler reduces the number of microvoids by filling them and results in the reduction of absorbed water and decrease in the diffusion coefficient.

CONCLUSIONS

Kinetic of DGEBA cured with DDA and DDA/NS by nonisothermal DSC technique with two methods, Ozawa and Kissinger was studied. The kinetic parameters, activation energy, pre-exponential factor, and rate constant were determined. The mechanism of cure reaction was studied by FTIR, and the con-

version curves against time for two systems were drawn. The initial slop in conversion curves for DGEBA/DDA/NS system was steeper than DGEBA/DDA system. It can be suggested from DSC data and mechanism of cure reaction in Scheme 2 that NS particles in DGEBA/DDA system acted as a catalyst and caused an increase in the rate of cure reaction. The existence of NS particles in DGEBA/DDA system also caused decrease in the activation energy and rate constant. Water diffusion measurement for the two systems showed that the diffusion coefficient decreases when NS particles are present. This is suggested to be because of the fact that nanosilical particles have acted as filler in filling the microvoids on the surface of the sample and therefore, less water can diffuse into the sample.

References

1. Alexander, M.; Balogh, L.; Gae, F.; Goettler, L.; Golovoy. In Proceedings of the Nanocomposites—Delivering New Value to Polymers, San Diego, CA, September, 23–25, 2002.
2. Lichtenhan, J. D., Otonari, Y. A., Carr, M. J. Macromolecules 1995, 28, 8435.
3. Pyun, J.; Matyjaszewski, K. Macromolecules 2000, 33, 217.
4. Kashiwagi, T.; Morgan, A. B.; Antonucci, J. M.; Vanlandingham, M. R.; Harris, R. H.; Awad, W. H.; Shields, J. R. J Appl Polym Sci 2003, 89, 2072.
5. Yu, Y. Y.; Chen, C. Y.; Chen, W. C. Polymer 2003, 44, 593.
6. Wang, Y. T.; Chang, T. C.; Hong, Y. S.; Chen, H. B. Thermochim Acta 2003, 397, 219.
7. Lin, J. J.; Cheng, I. J.; Wang, R.; Lee, R. J. Macromolecules 2001, 34, 8832.
8. Merkel, T. C.; Freeman, B. D.; Spontak, R. J.; He, Z.; Pinnau, I.; Meakin, P.; Hill, A. J. J Chem Mater 2003, 15, 109.
9. Lee, A.; Lichtenhan, J. D. Macromolecules 1998, 31, 4970.
10. Li, G. Z.; Wang, L.; Toghiani, H.; Daulton, T. L., Jr.; Pittman, C. U. Polymer 2002, 43, 4167.
11. Liu, Y.-L.; Hsu, C.-Y.; Wei, W.-L.; Jeng, R.-J. Polymer 2003, 44, 5159.
12. Abad, M. J.; Barral, L.; Fasce, D. P.; Williams, R. J. J. Macromolecules 2003, 36, 3128.
13. Horie, K.; Hiura, H.; Sawada, M.; Mita, I.; Kambe, H. J Polym Sci A 1970, 8, 1357.
14. Mijovic, J.; Kim, J.; Slaby, J. J Appl Polym Sci 1984, 29, 1449.
15. Deng, Y.; Martin, G. C. Macromolecules 1994, 27, 5147.
16. Girard-Rejdet, E.; Riccardi, C. C.; Sautereau, H.; Pasault, J. P. Macromolecules 1995, 28, 7599.
17. Ghaemy, M.; Sadjady, S. J Appl Polym Sci 2006, 100, 2634.
18. Pryde, C. A.; Hellman, M. Y. Polym Prepr (Am Chem Soc Div Polym Chem) 1979, 20, 620.
19. Apicella, A.; Nicolais, L.; Cataldis, C. Adv Polym Sci 1985, 66, 189.
20. Antoon, M. K.; Koenig, J. L. J Polym Sci Part B: Polym Phys 1981, 19, 197.
21. Apicella, A.; Nicolais, L.; Astarita, G.; Drioli, E. Polymer 1981, 22, 1064.
22. Diamant, Y.; Marom, G.; Broutman, L. J. J Appl Polym Sci 1981, 26, 3015.
23. McKague, E. L.; Reynolds, J. D., Jr.; Halkias, J. E. J Appl Polym Sci 1978, 22, 1643.
24. Bueche, F. Physical Properties of Polymers; Interscience: New York, 1962.
25. Couchmann, P. R.; Karasz, F. E. Macromolecules 1978, 11, 117.
26. Moy, P.; Karasz, F. E. Polym Eng Sci 1980, 20, 315.
27. Ivanova, K. I.; Pethrick, R. A.; Affrossman, S. Polymer 2000, 41, 6787.
28. Liu, Y. L.; Li, S. H. J Appl Polym Sci 2005, 95, 1237.
29. Kissinger, H. E. Anal Chem 1957, 29, 1702.
30. Gu, J., Narang, S. C.; Pearce, E. M. J Appl Polym Sci 1985, 30, 2997.
31. Ozawa, T. J Therm Anal Calorim 1970, 2, 301.
32. Moroni, A.; Mijovic, J.; Pearce, E.; Foun, C. C. J Appl Polym Sci 1986, 32, 3761.
33. Pethrick, R. A.; Hollins, E. A.; McEwan, I.; Pollock, E. A.; Hayward, D. Polym Int 1996, 39, 275.